Reprint Technical Note, Nuclear Science & Engineering: 75, 184-190 (1980)

Technical Notes

Effect of Photoneutrons on Thermalization Experiments in Deuterium

C. J. Gho, M. M. Sbaffoni, T. F. Parkinson,* and M. J. Abbate

Centro Atómico Bariloche, Comisión Nacional de Energía Atómica
8400 San Carlos de Bariloche (R.N.), Argentina

Received September 14, 1979
Accepted February 27, 1980

ABSTRACT

The neutron slowing down process is frequently studied by means of a pulsed-electron beam from a Linac impinging on a heavy metal target. The resulting pulses of photoneutrons are thermalized and the differential spectrum is measured via *the time-of-flight method. If the thermalizing medium contains deuterium or beryllium, a secondary distributed photoneutron source is produced by the gamma-ray flash from the Linac. The magnitude of this secondary source in D_2O was measured by foil activation and it was shown that the effect of the secondary source can be accurately evaluated.*

INTRODUCTION

When the electron beam from a Linac, in conjunction with an appropriate heavy metal target, is used as a pulsed-neutron source,[1] very intense high-energy bremsstrahlung radiation is also produced. In experiments involving D_2O, this radiation generates photoneutrons through the (γ,n) reaction in deuterium, with a threshold energy of 2.2 MeV (Ref. 2). Thus, a distributed secondary source of photoneutrons is created in the D_2O, which adds to the primary

*Permanent address: Nuclear Engineering Group, Virginia Polytechnical Institute and State University, Blacksburg, Virginia 24061.

[1]M. J. ABBATE, J. V. LOLICH, and T. F. PARKINSON, *Nucl. Sci. Eng.*, **60**, 471 (1976).

[2]H. F. BOWSHER et al., "Photoneutron Cross Sections for D_2O and Beryllium," DP-MS-75-95, Savannah River Laboratory (1975).

neutron source formed from the target. Both primary and secondary sources are fast neutrons but with different spatial and energy distributions, so the measured total neutron flux will not show the expected relaxation effect and thus will result in a modification in the transverse buckling value to be used to correct for leakage in one-dimensional calculations. If this secondary source is not considered in the comparisons between measured and calculated spectra in D_2O, some discrepancies could arise that might explain observed differences.[3,4] Similar effects would also occur in experiments with beryllium when a Linac source is used.

In this paper, we present the measurement of the secondary source effect in D_2O and the possibility of representing the total source from calculated spatial distributions of its components.

EXPERIMENTS

Considering the difficulty of directly measuring the gamma-ray flux due to the extremely intense and high-energy bremsstrahlung, the most obvious way to perform the experiments is to measure the epithermal spatial distribution of the neutron population [i.e., $\phi(E,r)$] in D_2O with both primary and secondary sources present, and then to repeat the measurement with one of the sources removed. The aim of the experiment consists, then, in the relative determination of the sources' effects without absolute measurements.

The experiment can be performed by two methods:

1. Subtracting the secondary source. It is possible either to include an adequate gamma-ray filter or to irradiate the assembly in the direction perpendicular to the electron beam that is the predominant axis of the gamma rays. In the first case, the primary source will also be strongly attenuated, and, in the second case, the primary source will undergo changes in several parameters that will complicate the comparisons, for example, modifications due to its anisotropic distribution.

2. Subtracting the primary source. This effect can be obtained using a low-efficiency neutron target (carbon, aluminum, beryllium), but in this case monitors will be necessary for the gamma-ray source, and these pose a very difficult problem because of the characteristics of this source. An alternative method is to include a low-mass neutron filter that will not significantly change the gamma-ray source.

This latter method was selected and the experimental arrangement is shown in Fig. 1. Basically, the geometry comprised a cylindrical stainless-steel tank (*B*) 50 cm long and 36 cm in diameter lined with a cadmium sheet and shielded with a boron mixture. The tank was filled with D_2O (99.5 mol% pure); a rectangular vessel 20 cm thick (*A*) filled with a boric acid in light water solution (60 g/ℓ) served as the neutron filter. The vessel *A* and the cylinder *B* were separated by a 2-mm-thick cadmium layer. The target was lead.

With respect to prior studies,[4] the secondary source was magnified and the primary source was minimized by introducing the following changes: the target reflector and a lead filter (2.5 cm thick) were removed. In this way, taking into account earlier experimental data, a ratio of ~1.3:1 between secondary and primary sources was expected. This ratio is adequate to give definitive results about the magnitude of the secondary source.

Spatial distributions of the epithermal neutron flux along the axis of the D_2O cylinder, ϕ and ϕ_f, respectively, were measured, first without the filter (vessel A empty), and then with the filter. The detectors were 0.254-mm-thick indium foils shielded by 0.5-mm-thick cadmium.

To obtain adequate spatial resolution (2 cm) and to prevent flux perturbations, the foils were spaced 4 cm apart,

[3]M. J. ABBATE, "Espectros del Flujo Angular de Neutrones cerca de una Interfase entre H_2O y D_2O," PhD Thesis, Instituto Balseiro, Universidad Nacional de Cuyo, Bariloche, Argentina (1977).

[4]M. J. ABBATE and J. V. LOLICH, *Atomkernenergie*, **33**, 195 (1979).

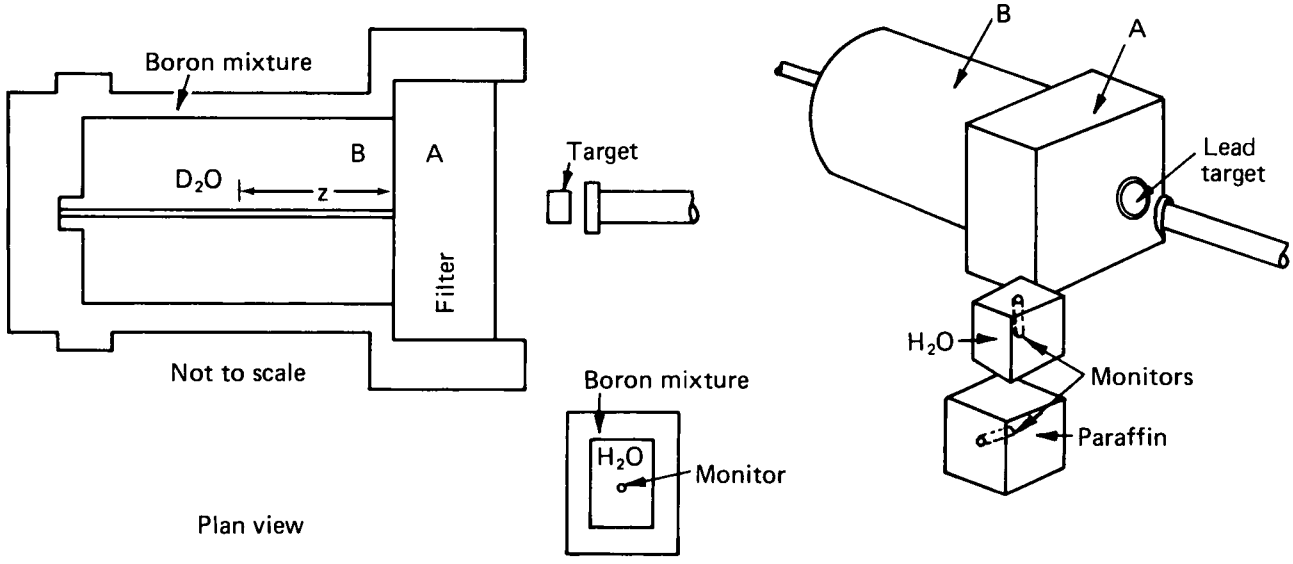

Fig. 1. Experimental arrangement to measure the secondary source in D_2O.

and then the measurement was repeated with the foil positions shifted by 2 cm.

A careful monitoring of the primary source was necessary to obtain correct normalization between the measurements. For this purpose, it was not possible to locate the detectors inside the geometry due to the strong changes in the neutron fields within the filter; thus, two auxiliary vessels were located near the target: a 12- X 18- X 18-cm^3 container of water and a 20- X 20- X 20-cm^3 cube of paraffin. In the middle of each vessel a miniature ^{235}U fission chamber was installed (see Fig. 1). The output of these detectors was gated closed just after the neutron pulse to eliminate initial saturation and also, in the pulse tail, to eliminate the backscattered neutrons entering the assembly.

For the irradiations, a deflected Linac electron beam was used; this way, the electron energy was constant and no changes due to this parameter could affect the gamma-ray spectrum; thus, the monitor responses were proportional only to the primary neutron source.

The irradiations were performed at a 100 pulse/s rate and included 500 000 Linac pulses. The estimated error for the monitors was 7%.

Table I shows the experimental results, in arbitrary units, and the ratio

$$R_m = \frac{\phi_f}{\phi} .$$

TABLE I

Experimental Values of the Epithermal Neutron Flux Along the Axis of the D_2O Cylinder (arbitrary units)

Position Along Axis of the D_2O Cylinder z (cm)	$\phi(z)$	$\phi_f(z)$	$R_m = \frac{\phi_f}{\phi}$
0.5	3.65	3.26	0.89
2.5	4.80	3.80	0.79
4.5	5.85	4.26	0.73
6.5	6.58	4.64	0.71
8.5	7.05	4.84	0.69
10.5	7.35	4.93	0.67
12.5	7.48	4.94	0.66
14.5	7.50	4.93	0.66
16.5	7.40	4.84	0.65
18.5	7.15	4.69	0.66
20.5	6.85	4.52	0.66
22.5	6.48	4.33	0.67
24.5	6.13	4.11	0.67
26.5	5.70	3.89	0.68
28.5	5.30	3.63	0.68
30.5	4.93	3.31	0.67
32.5	4.53	3.14	0.69
34.5	4.13	2.90	0.70
36.5	3.78	2.64	0.70
38.5	3.42	2.39	0.70
40.5	3.08	2.17	0.70
42.5	2.73	1.91	0.70
44.5	2.39	1.69	0.71
46.5	2.05	1.48	0.72
48.5	1.72	1.28	0.74

These values are estimated to have a 10% minimum relative error.

From these data and their representation in Fig. 2, it is possible to see that the filter resulted in a 2-cm displacement of the maximum in the epithermal distribution (from z = 14.5 cm to z = 12.5 cm) due to the neutron moderation in the filter, a 34% decrease in the maximum, and a 30% decrease at z = 40.5 cm.

In this case, where, as will be shown later, the primary source is 99% attenuated by the filter, the attenuation of the total flux is lower and its slope is changed by 14% (see Fig. 2).

The relaxation constants calculated from the data in the region of spectrum equilibrium, that is, between z = 18.5 and 34.5 cm, were: $\gamma^2 = -0.00118$ cm^{-2} without the filter and $\gamma^2 = -0.00090$ cm^{-2} with the filter. This result shows the importance of the leakage corrections of the calculations.

CALCULATIONS

The results of the measurements can be interpreted in the following way. The total flux is due to the contributions of the primary and secondary sources. Thus, in the no-filter case:

$$\phi(z) = S_p \phi_p(z) + S_s \phi_s(z) , \quad (1)$$

where

$\phi_p(z)$ and $\phi_s(z)$ = spatial epithermal neutron distributions due to the primary and secondary sources, respectively, when one fast neutron is introduced in the system, with the corresponding energy spectrum

S_s and S_p = fast neutron intensities.

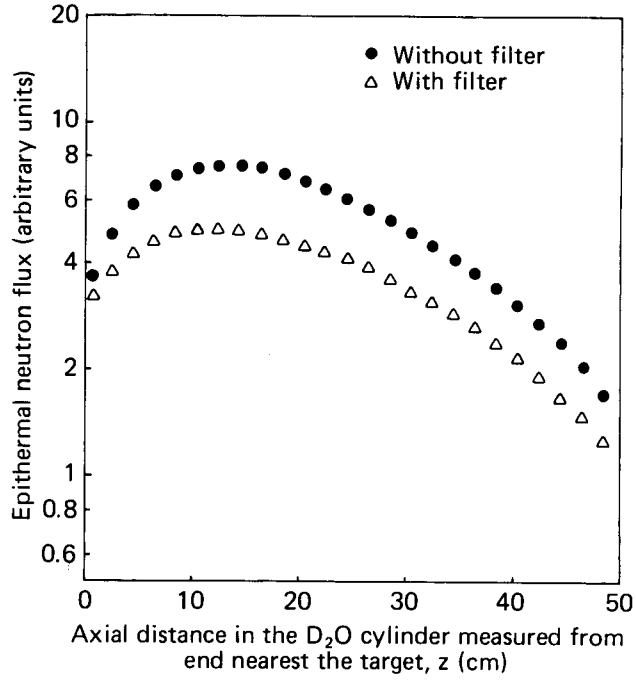

Fig. 2. Experimental values of neutron flux.

In the measurements with the filter,

$$\phi_f(z) = S'_p\phi'_p(z) + S'_s\phi'_s(z) \ , \qquad (2)$$

where the functions have the same meaning, and

$$\epsilon_p S_p = S'_p \ ,$$
$$\epsilon_s S_s = S'_s \ ,$$

where

ϵ_p = neutron transmission of the filter

ϵ_s = gamma-ray transmission of the filter.

To reproduce these components, one-dimensional calculations were made using the NYR 235-ANISN code[5] to obtain the spatially dependent neutron fluxes $\phi_p(z)$, $\epsilon_p\phi'_p(z)$, $\phi_s(z)$, and $\phi'_s(z)$, and, from these, the activation of indium foils for epicadmium energies.

Group constants were derived from the GGC-3 neutron cross-section library[6] in 34-energy groups. Also 66 spatial intervals in the axial direction and the P_0 and S_6 approximations were used in the calculations. The energy mesh was selected to have a detailed description in the epithermal range. Moreover, the program contained four fast groups, where the real neutron source is included, and seven thermal groups.

Radial leakage was corrected by a geometrical buckling factor according to earlier results.[4] However, no good agreement with experimental data was expected near boundaries and interfaces.

Four cases were calculated, corresponding to the four unknown z functions in Eqs. (1) and (2). Thus, for the primary flux determination, the geometry of Fig. 1 was calculated with and without the filter using a unitary fast neutron source located 2.5 cm in front of vessel A. These calculations gave as results $\phi_p(z)$ and $\epsilon_p\phi'_p(z)$, respectively. The spectrum of the source was obtained from the energy dependent (γ,n) cross section of the lead target[7] in conjunction with the bremsstrahlung spectrum calculated with Schiff's expression[8] corresponding to lead and 25-MeV electrons.[9]

For the secondary flux determination, the above calculations were repeated, but with a unitary fast neutron source distributed along the axis of the D_2O cylinder and zero value within the filter to obtain $\phi_s(z)$ and $\phi'_s(z)$. The secondary source energy spectrum follows from the bremsstrahlung spectrum of the lead target and the energy-dependent (γ,n) cross section of deuterium.[2]

Actually this source has a spatial dependence due to gamma-ray attenuation in heavy water; this factor was taken into account by using an exponential form with a relaxation constant of 0.021 cm^{-1} derived from the energy attenuation factor in light water. This constant corresponds to 5-MeV photons. However, no differences >1% were found in the neutron fluxes between this calculation and others using the constants 0.15 and 0.25 cm^{-1} for 20 and 2 MeV, respectively. Moreover, slight changes in the source spectra did not significantly alter the results. These theoretical results are included in Table II and Fig. 3, only for the D_2O region, for the sake of simplicity.

The magnitude of ϵ_s has been approximated by

$$\epsilon_s = \frac{\int_{2.2}^{\infty} B(E)\exp[-\lambda(E)x]dE}{\int_{2.2}^{\infty} B(E)dE} \ ,$$

where

$B(E)$ = bremsstrahlung spectrum

$\lambda(E)$ = attenuation coefficient

x = filter thickness.

The value obtained is $\epsilon_s = 0.7$.

From the ratios between the results of the first two calculations, it follows that the neutron transmission of the filter (ϵ_p) is ~0.011, disregarding the spatial dependence; the maximum of the distribution appears to be displaced 2 cm toward the target by the moderation effect.

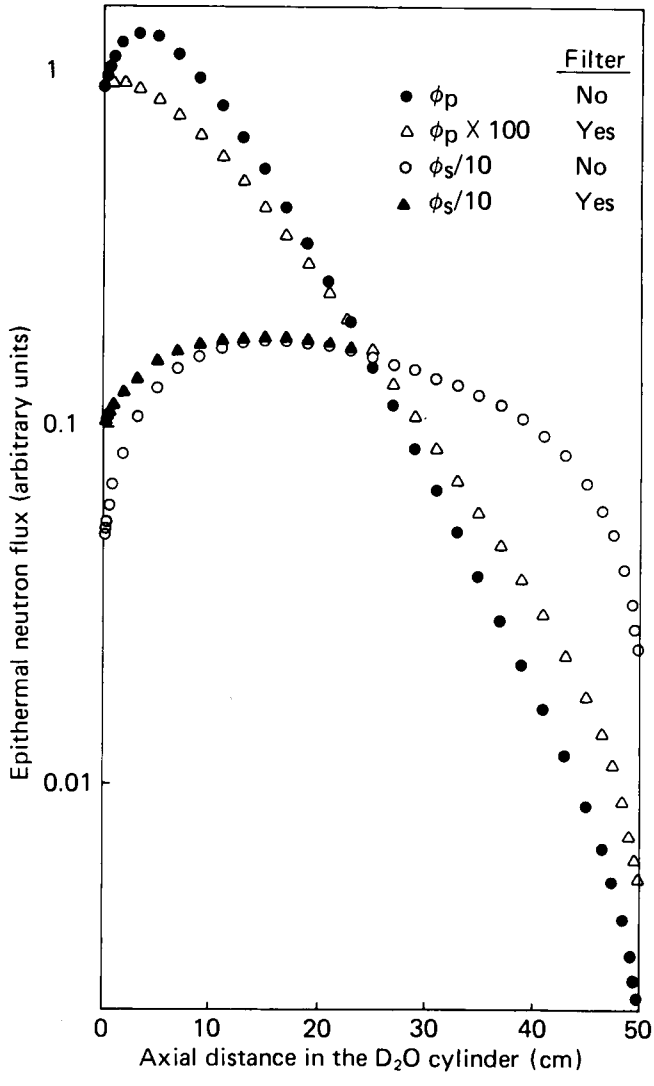

Fig. 3. Theoretical primary and secondary epithermal fluxes.

[5]C. J. GHO, "NYR 235-Versión Local del Programa ANISN," Archivo Computacional de la División Neutrónica y Reactores, Centro Atómico Boriloche, Argentina (1976).

[6]H. J. BOADO et al., "Production of Multigroup Cross Section Sets from GGC-3 Data Library," OECD-NEA Newsletter No. 22, Organization for Economic Cooperation and Development (1977).

[7]R. MONTALBETTI et al., *Phys. Rev.*, **91**, 659 (1953).

[8]J. GOLDEMBERG and L. KATZ, *Can. J. Phys.*, **32**, 49 (1954).

[9]Note that in the case with filter, the calculated primary flux distribution is already affected by the ϵ_p factor, and this factor would be equal to R if there were no secondary source present.

TABLE II

Calculated Values of the Neutron Flux Along the Axis of the D_2O Cylinder (arbitrary units)

Position Along Axis of the D_2O Cylinder z (cm)	Primary Source $\phi_p(z)$			Secondary Source $\phi_s(z)$		
	No Filter	Filter	Ratio	No Filter	Filter	Ratio
0.01	8.999-1[a]	9.168-3	0.010	4.920-1	1.039	2.11
0.04	9.086-1	9.173-3	0.010	4.992-1	1.043	2.09
0.10	9.255-1	9.185-3	0.010	5.133-1	1.051	2.05
0.22	9.574-1	9.203-3	0.010	5.412-1	1.067	1.97
0.45	1.012	9.231-3	0.009	5.926-1	1.096	1.85
0.90	1.098	9.251-3	0.008	6.866-1	1.151	1.68
1.75	1.202	9.192-3	0.008	8.445-1	1.246	1.48
3.15	1.265	8.906-3	0.007	1.062	1.382	1.30
5.0	1.228	8.303-3	0.007	1.288	1.527	1.19
7.0	1.109	7.486-3	0.007	1.468	1.642	1.12
9.0	9.560-1	6.601-3	0.007	1.592	1.719	1.08
11.0	7.994-1	5.721-3	0.007	1.671	1.763	1.06
13.0	6.537-1	4.893-3	0.007	1.713	1.781	1.04
15.0	5.256-1	4.139-3	0.008	1.728	1.777	1.03
17.0	4.169-1	3.472-3	0.008	1.722	1.757	1.02
19.0	3.272-1	2.891-3	0.009	1.699	1.724	1.01
21.0	2.546-1	2.394-3	0.009	1.663	1.682	1.01
23.0	1.967-1	1.973-1	0.010	1.619	1.632	1.01
25.0	1.512-1	1.620-3	0.011	1.567	1.577	1.01
27.0	1.156-1	1.326-3	0.011	1.510	1.517	1.01
29.0	8.812-2	1.083-3	0.012	1.448	1.453	1.00
31.0	6.696-2	8.820-4	0.013	1.382	1.385	1.00
33.0	5.075-2	7.165-4	0.014	1.310	1.313	1.00
35.0	3.838-2	5.805-4	0.015	1.234	1.236	1.00
37.0	2.894-2	4.684-4	0.016	1.150	1.151	1.00
39.0	2.175-2	3.758-4	0.017	1.057	1.058	1.00
41.0	1.625-2	2.986-4	0.018	9.536-1	9.523-1	0.99
43.0	1.200-2	2.334-4	0.019	8.355-1	8.360-1	1.00
45.0	8.671-3	1.771-4	0.020	6.990-1	6.994-1	1.00
46.50	6.558-3	1.385-4	0.021	5.841-1	5.843-1	1.00
47.50	5.326-3	1.142-4	0.021	4.967-1	4.969-1	1.00
48.50	4.148-3	8.982-5	0.022	3.933-1	3.994-1	1.00
49.25	3.271-3	7.110-5	0.022	3.190-1	3.192-1	1.00
49.65	2.794-3	6.066-5	0.022	2.721-1	2.722-1	1.00
49.90	2.487-3	5.389-5	0.022	2.410-1	2.411-1	1.00

[a] Read as 8.999×10^{-1}.

With respect to the second two calculations, these results agree to within 1% in the equilibrium spectrum zone, i.e., between z = 19 and 34 cm; it is, therefore, possible to assume that in this region $\phi_s(z) = \phi'_s(z)$. For lower z values the distribution with the filter is a factor of 2 larger than that without the filter. The explanation of this change is that part of the neutron leakage into the filter tank is moderated and reflected into the heavy water.

DISCUSSION OF RESULTS

From these preliminary results the experimental and theoretical values can be combined to obtain the distributed total flux from its calculated components.

Using numerical regression by minimum quadratures in the expression:

$$\phi(z) = \alpha\phi_p(z) + \beta\phi_s(z) \ ,$$

where $\phi(z)$ are experimental values (Table I) and $\phi_p(z)$ and $\phi_s(z)$ are calculated values (Table II), the following were obtained:

$$\alpha = 2.66 \pm 0.53 \ ,$$

$$\beta = 3.43 \pm 0.17 \ .$$

Thus,

$$\frac{\beta}{\alpha} = \frac{S_s}{S_p} = 1.29 \ . \qquad (3)$$

No points close to the boundary were used in this regression analysis. Had the equilibrium zone been larger, the fitting, and consequently the results, would have been better.

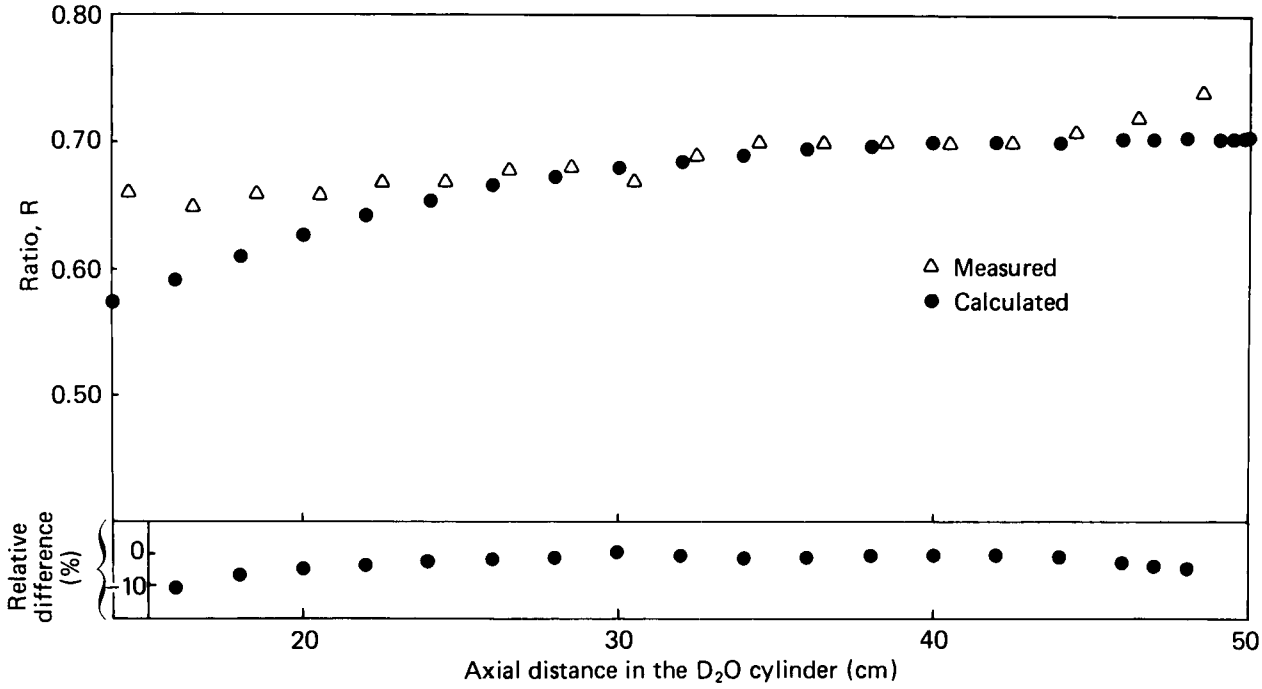

Fig. 4. Ratios between total epithermal fluxes with and without filter.

It is easy to verify from the estimated values for $\epsilon_p\phi'_p(z)$ and $\epsilon_s\phi'_s(z)$ that it makes no sense to try to perform a numerical regression in the expression $\alpha\epsilon_p\phi'_p(z) + \beta\epsilon_s\phi'_s(z) = \phi_f(z)$ because the values of $\alpha\epsilon_p\phi'_p(z)$ would be smaller than the estimated errors in $\phi_f(z)$.

As a test of the validity of Eq. (3), with this normalization, the R ratio can be obtained from the calculated distributions by

$$R(z,\epsilon_s) = \frac{\alpha\epsilon_p\phi'_p(z) + \beta\epsilon_s\phi'_s(z)}{\alpha\phi_p(z) + \beta\phi_s(z)} . \qquad (4)$$

Calculating $R(z,\epsilon_s)$ for different values of ϵ_s yields an asymptotic value equal to ϵ_s for large z values. This result can be anticipated from Eq. (4) when the secondary source contribution is important as in the present case ($\beta/\alpha = 1.29$).

Then it is possible to obtain a refined value for ϵ_s from the measurements, namely, 0.70 in agreement with the estimations, because this is the asymptotic value of R_m for large z. Resulting values of R are included in Table III and represented in Fig. 4 together with R_m. The value of $\epsilon_s = 0.70$ implies that the average gamma-ray energy can be taken as 8 MeV.

In general, the z dependence of these ratios was expected from the behavior of its components, but there are significant differences from those expectations. In the final 6 cm beyond the equilibrium zone, a deviation of −4% was found. In this region, R_m increases faster than R as a consequence of boundary effects not important in this problem. Furthermore, for $z < 25$ cm, $R_m > R$. This is the zone where the calculated fluxes are importantly affected by the filter; perhaps the effect of the filter was not totally reproduced by the calculations. At any rate, the largest relative difference in the equilibrium zone is only −6%.

Calculations of R were repeated with different β/α

TABLE III

Ratio Between Total Epithermal Neutron Fluxes With and Without the Filter, R

Position Along Axis of D_2O Cylinder z (cm)	R
10.0	0.525
12.0	0.548
14.0	0.571
16.0	0.591
18.0	0.611
20.0	0.628
22.0	0.643
24.0	0.655
26.0	0.666
28.0	0.673
30.0	0.681
32.0	0.686
34.0	0.691
36.0	0.695
38.0	0.697
40.0	0.700
42.0	0.700
44.0	0.702
46.0	0.703
47.0	0.704
48.0	0.704
49.0	0.704
49.5	0.704
49.8	0.704
50.0	0.704

ratios and these have shown that when $\beta/\alpha \leqslant 0.25$, R is more sensitive to z, thus facilitating its experimental determination.

CONCLUSIONS

From these measurements it was possible to evaluate the secondary photoneutron source in D_2O in experiments that involve the use of a strong gamma-ray source. It was shown, too, that it is possible to represent the measured total flux by its calculated components and to obtain in this way the spatial distribution of the secondary flux. With respect to actual cases where this secondary source can be 20% or less of the primary source, it was shown that the method we described will be adequate to take into account its effects.

To achieve higher accuracy, the calculations should be improved, perhaps including anisotropic scattering to remove the discrepancies close to the filter, and a more precise monitoring system should be provided. Nevertheless, the method has been proved to be valid, recalling that its most interesting feature is its simplicity.

ACKNOWLEDGMENT

This work was done under the auspices of CONICET and was supported by a grant from the U.S. National Science Foundation.